

Piezoresistance and Piezo-Hall Effects in *n*-ZnSe

A. SAGAR

Westinghouse Research Laboratories, Pittsburgh, Pennsylvania 15235

M. POLLAK

Department of Physics, University of California, Riverside, California 92502

AND

W. LEHMANN

Westinghouse Research Laboratories, Pittsburgh, Pennsylvania 15235

(Received 6 June 1968)

Large piezoresistance and piezo-Hall effects were observed in *n*-ZnSe samples. The experimental result for the shear piezoresistance coefficient, $\pi_{shear} \approx 0$, is consistent with the model that the lowest conduction-band minimum for this material lies at $\mathbf{k} = (0,0,0)$. The large piezoresistance and piezo-Hall effects can be qualitatively explained on the basis of the large pressure dependence of the donor ionization energy ϵ_d . The data on the longitudinal coefficient $\pi_l(\rho)$ versus T give a value $\epsilon_d \approx 0.019$ eV, in excellent agreement with the value $\epsilon_d \approx 0.020$ eV estimated from the low-temperature data on the resistivity ρ versus T . The result $(d\epsilon_d/dP) \geq +5.2 \times 10^{-12}$ eV/dyn cm⁻² was obtained from the pressure data at 195°K, and suggests that there is considerable contribution from some band other than the (0,0,0) conduction band to the donor state functions. The piezoresistance data around 20°K, when simply interpreted on the basis of the pressure dependence of the ionization energy of the single donor level, gave the value $(d\epsilon_d/dP) \approx +2.6 \times 10^{-12}$ eV/dyn cm⁻², in disagreement with the estimate obtained from the pressure data at 195°K.

1. INTRODUCTION

THE band structure of ZnSe has been investigated by various workers. Edwards *et al.*¹ studied the effect of hydrostatic pressure on the absorption edge of ZnSe. They find an initial blue shift with a slope of $d(\Delta E_g)/dP = +6 \times 10^{-12}$ eV/dyn cm⁻² at atmospheric pressure. The maximum blue shift is 0.49 eV at 1.3×10^{11} dyn/cm²; it is followed by a red shift with a slope of $d(\Delta E_g)/dP = -2 \times 10^{-12}$ eV/dyn cm⁻². Following the work of Paul and Warschauer² on the systematics of the pressure dependence of the band edges of the zinc-blende structure semiconductors, it could be concluded that for ZnSe the lowest conduction-band minimum lies at $k = (000)$, and the next higher minima lie along the [100] directions in k space, at about 0.75 eV above the lowest minimum. The (000) conduction band for ZnSe is also suggested by various optical experiments.^{3,4} Marple⁵ measured the infrared reflectance and Faraday rotation for *n*-ZnSe samples and obtained a value for the electron effective mass $m^* = (0.17 \pm 0.025)m_e$ for this material. The electrical properties of *n*-ZnSe were first measured by Aven and Segall.⁶ The samples used in their work were single crystals prepared from the General Electric Chemical Products Plant ZnSe powder. The crystals were grown by the technique described by Piper and Polich.⁷ The samples were subjected to the

purification technique in which the crystals were heated in contact with molten Zn at 900°C for a few days. They succeeded in preparing *undoped low-resistivity n*-ZnSe samples [$\rho(300^\circ\text{K}) \approx 1 \Omega\text{cm}$] by this technique. They were further able to prepare degenerate *n*-ZnSe samples ($n \approx 1.5 \times 10^{20}$ cm⁻³) by diffusing Al into a previously purified ZnSe crystal.

This paper reports some results of our investigations on the effect of (1) hydrostatic pressure and (2) uniaxial stress on the Hall coefficient and resistivity of extrinsic *n*-ZnSe samples. The Hall coefficient and resistivity of the samples were measured up to 10^{10} dyn/cm² at 300 and 195°K. The effect of uniaxial stress on the Hall coefficient and resistivity of these samples was measured between 77° and 300°K; the piezoresistance measurements on one of the samples were made down to 20.4°K.

2. EXPERIMENT

2.1 Material and Sample Preparation

The ZnSe powder was obtained from General Electric Chemical Products Division. The powder was purified by fractional sublimation method, somewhat similar to the method described by Vecht *et al.*⁸ for CdS. The crystals were grown by the method of Piper and Polich.⁷ The crystals always contained a large number of twins. However, large portions of the ingot contained twins of similar composition, i.e., with all the twin planes parallel. Samples were cut so that they contained only parallel twin planes (Fig. 1). The dimensions of the samples were approximately $12 \times 2 \times 2$ mm. The crystallographic orientations of the samples used are shown in Fig. 1. The samples in Fig. 1(a) have the (111) twin planes normal to the long dimension of the sample. Thus

¹ A. L. Edwards, T. E. Slykhouse, and H. G. Drickamer, *J. Phys. Chem. Solids* **11**, 140 (1959).

² W. Paul and D. M. Warschauer, *Solids Under Pressure* (McGraw-Hill Book Co., New York, 1963), p. 179

³ M. Aven, D. T. F. Marple, and B. Segall, *J. Appl. Phys.* **32**, 2261 (1961).

⁴ B. Segall, *Physics and Chemistry of II-VI Compounds*, edited by M. Aven and J. S. Prener (North-Holland Publishing Co., Amsterdam, 1967), p. 50.

⁵ D. T. F. Marple, *Phys. Rev.* **35**, 1879 (1964).

⁶ M. Aven and B. Segall, *Phys. Rev.* **130**, 81 (1963).

⁷ W. W. Piper and S. J. Polich, *J. Appl. Phys.* **32**, 1278 (1961).

⁸ A. Vecht, B. W. Ely, and A. Apling, *J. Electrochem. Soc.* **111**, 666 (1964).

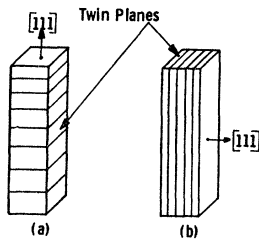


FIG. 1. The crystallographic orientations of the samples and the configuration of the twins present in the samples.

the crystallographic direction of the long dimension of these samples is completely defined; it is the $[111]$ direction. Such samples will be referred to as the $[111]$ samples. The long dimension of the samples of the type shown in Fig. 1(b) do not have a unique crystallographic orientation for the whole sample. However, the direction of the long dimension of these samples lies in the (111) plane for any portion of the sample. Such samples will be referred to as the (111) samples.

The samples were subjected to the purification technique described by Aven and Segall.⁶ The following procedure was found suitable for making low-electrical-resistance contacts to the samples. The samples were lapped and etched in either a solution of bromine and methanol or in hot HCl. Indium was first soldered to the samples with the ultrasonic soldering tip. The samples were then fired at about 250 to 300°C in hydrogen atmosphere for about 5 min. However, it was later found that firing of the samples in the hydrogen atmosphere is not essential for obtaining low-resistance contacts. Equally good low-resistance contacts could be obtained by *prolonged* application of indium with the ultrasonic soldering tip.

2.2 Sample Characterization

The samples are characterized by their resistivity and Hall-coefficient values given in Table I. The two Hall-coefficient values for each sample shown in the table are the values at two points about 8 mm apart along the length of the samples, and reflect the inhomogeneity in the samples. The resistivity values measured at two sets of probes were generally the same within 10%. The electron mobility μ_H for the samples was calculated by using the average value for R_H for each sample. All electrical measurements were made in dark to avoid photoexcitation.

2.3 Piezoresistance and Piezo-Hall Measurements

A. Longitudinal Piezoresistance

The longitudinal piezoresistance measurements (with current and the stress along the long dimension of the samples) were made along two different crystallographic orientations using samples of the types shown in Fig. 1. These measurements were made between 77 and 300°K. Measurements on sample No. 7 were made down to 20.4°K.

The fractional change of resistivity $(\Delta\rho/\rho)$ due to applied stress X (with current and stress in the same direction) in terms of the fractional change of resistance $(\Delta R/R)$ of the sample, and the three piezoresistance coefficients π_{11} , π_{12} , π_{44} , is given by⁹

$$\begin{aligned} (\Delta\rho/X\rho)_{l,m,n} &= \pi_{11} - 2(\pi_{11} - \pi_{12} - \pi_{44})(l^2m^2 + m^2n^2 + n^2l^2) \\ &= (\Delta R/RX)_{l,m,n} + [(S_{11} + 2S_{12}) - 2S_{11}'], \end{aligned}$$

where $S_{11}' = S_{11} - 2(S_{11} - S_{12} - \frac{1}{2}S_{44})(l^2m^2 + m^2n^2 + n^2l^2)$. The coefficients l , m , and n are the direction cosines of specimen axis, which is also the direction for the current and the stress. The coefficients S_{11} , S_{12} , and S_{44} are the elastic compliances for ZnSe, and have been measured by Berlincourt *et al.*¹⁰ The measurements on the $[111]$ -type samples would yield

$$(\Delta\rho/X\rho)_{[111]} = \frac{1}{3}(\pi_{11} + 2\pi_{12}) + \frac{2}{3}\pi_{44}.$$

The quantity $(l^2m^2 + m^2n^2 + n^2l^2) = \frac{1}{4}$ for any direction lying in the (111) plane.¹¹ Thus the longitudinal piezoresistance measurements made on the (111) -type samples yields

$$(\Delta\rho/X\rho)_{(111)} = \frac{1}{3}(\pi_{11} + 2\pi_{12}) + \frac{1}{6}[3\pi_{44} + (\pi_{11} - \pi_{12})],$$

where the subscript (111) refers to any direction lying in the (111) plane.

No transverse piezoresistance measurements (with the stress perpendicular to the current direction) were made because of the difficulty of making low-resistance contacts on large areas of the samples. Instead, the resistance of the samples was measured as a function of hydrostatic pressure to complete the information on the three piezoresistance coefficients. The hydrostatic pressure measurements were made only at 195 and 300°K. The maximum pressure used was 10¹⁰ dyn/cm².

B. Resistance versus Hydrostatic Pressure

The effect of hydrostatic pressure P on the resistivity of the samples in terms of the π 's is given by

$$\begin{aligned} d(\ln\rho)/dP &= (\pi_{11} + 2\pi_{12}) \\ &= d(\ln R)/dP + (S_{11} + 2S_{12}). \end{aligned}$$

The value of $(\pi_{11} + 2\pi_{12})$ at $P=0$ was derived from the slope of the curves for resistance versus pressure at $P=0$. Thus the resistance-versus-pressure data along with the piezoresistance measurements for the two orientations gives complete information on the dilatational component $(\pi_{11} + 2\pi_{12})$ and the two shear components π_{44} and $(\pi_{11} - \pi_{12})$ of the piezoresistance tensor.

⁹ R. F. Potter and W. J. McKean, *J. Res. Natl. Bur. Std. (U. S.)* **59**, 427 (1957); J. F. Nye, *Physical Properties of Crystals* (Oxford University Press, London, 1960), p. 145.

¹⁰ D. Berlincourt, H. Jaffe, and L. R. Shiozawa, *Phys. Rev.* **129**, 1009 (1963).

¹¹ The direction cosines of any direction normal to the $[111]$ direction are given by the equations $l+m+n=0$ and $l^2+m^2+n^2=1$. Thus $l^2m^2+m^2n^2+n^2l^2 = \frac{1}{4}$ for any direction lying in the (111) plane.

TABLE I. Hall coefficient and resistivity of n -ZnSe samples. The two values of the Hall coefficient for each sample are the values measured at two points about 8 mm apart along the length of the sample and represent the inhomogeneity in our samples. The resistivity values measured at the two sets of probes were generally the same within 10%. The electron mobility μ_H was calculated by using the average value for R_H for each sample. All electrical measurements were made in the dark to avoid photo excitation.

Sample No. and orientation of the sample axis	77°K			195°K			300°K		
	$-R_H$ ($\text{cm}^2 \text{C}^{-1}$)	ρ (Ωcm)	$\mu_H = (R_H/\rho)$ $\text{cm}^2 \text{V}^{-1} \text{sec}^{-1}$	$-R_H$ ($\text{cm}^2 \text{C}^{-1}$)	ρ (Ωcm)	$\mu_H = (R_H/\rho)$ $\text{cm}^2 \text{V}^{-1} \text{sec}^{-1}$	$-R_H$ ($\text{cm}^2 \text{C}^{-1}$)	ρ (Ωcm)	$\mu_H = (R_H/\rho)$ $\text{cm}^2 \text{V}^{-1} \text{sec}^{-1}$
2 [111]	3.91×10^4 6.45×10^4	32.7	1584	1.62×10^4 2.33×10^4	30	655	1.09×10^4 1.54×10^4	39	338
4 (111)	9.95×10^4 1.66×10^5	57.2	2321	2.12×10^4 3.35×10^4	33.3	823	1.42×10^4 2.2×10^4	41.5	436
7 (111)	4.3×10^3 6.2×10^3	3.3	1590	1.2×10^3 1.4×10^3	1.61	807	1.02×10^3 1.18×10^3	2.26	487

C. Hall Coefficient versus Hydrostatic Pressure and Piezo-Hall Measurements

The effect of hydrostatic pressure on the Hall coefficient of the samples was measured along with the measurements on resistance versus pressure, in order to determine if the observed large dependence of resistance of n -ZnSe on hydrostatic pressure is associated with any large changes in the electron mobility as a function of hydrostatic pressure.

The piezo-Hall coefficient

$$\pi_l(R_H) = [R_H(X) - R_H(0)] / X R_H(0)$$

was measured along with the longitudinal piezoresistance effect on some of the samples between 77 and 300°K. The subscript l refers to the case when both the current and the stress are along the same direction, which is also the direction of the long dimension for our samples.

D. Apparatus Used for Piezoresistance and Piezo-Hall Measurements

The method used for the piezoresistance measurements between 77 and 300°K was similar to that used by Pollak.¹² The samples were subjected to an alternating stress (27 cps) of the order of 5×10^7 dyn/cm². The over-all uncertainty in the experimental values of π_l 's was $\pm 2\%$ or $\pm 0.5 \times 10^{-12}$ cm²/dyn, whichever is larger. Furthermore, this method measures the adiabatic piezoresistance coefficients which should be converted to the isothermal values before comparing them with the results from hydrostatic pressure measurements, which are made under isothermal conditions. The difference between the isothermal and the adiabatic coefficients was estimated to be quite small¹² ($\approx 10^{-12}$ cm²/dyn) and was neglected.

The same apparatus was used for piezo-Hall measurements. The application of the alternating stress on the sample results in vibrations of the sample and the electrical leads relative to the magnetic field; this induces a voltage $= e(d/dt) \int \mathbf{H} \cdot d\mathbf{A}$ in the leads where

$d\mathbf{A}$ refers to the area of the loops formed by the flexible leads. This induced voltage reverses phase on reversing the direction of the magnetic field; it is, however, independent of the current. The piezo-Hall voltage reverses phase on reversing the direction of the magnetic field or the current. Thus the induced voltage can be eliminated by averaging (with proper phases) the measurements obtained for the two current directions. The induced voltage can be directly measured by turning the current off, and can be subtracted from the measured voltages on the Hall electrodes (taking into account the relative phases) for the two current directions. However, it is best to eliminate it. The following precautions were taken to eliminate it: (1) The leads were very well twisted together, thus making $d\mathbf{A}/dt = 0$; (2) the system was made more rigid. This was done by using a glass rod rather than the stainless steel tubing used in Pollak's work¹² for transmitting the stress.

The piezoresistive voltage, which appears due to misalignment of the Hall electrodes, is independent of the magnetic field, and can be eliminated by averaging (with proper phases) the two measurements obtained for the two magnetic field directions.

The following procedure was followed to obtain the piezo-Hall coefficient: The zero-stress Hall voltage V_{Hdc} was first measured in the usual way by averaging the four measurements for the four combinations of current and field directions. The alternating stress was then applied (with the same current and field) which causes an alternating voltage to appear across the Hall electrodes; this alternating voltage is the sum of piezoresistance and piezo-Hall voltage. A compensating voltage (from the oscillator which activates the alternating stress) of adjustable phase and amplitude was added in series to cancel the ac signal across the Hall electrodes. The magnetic field was then reversed. The ac voltage V_{Hac} across the Hall electrodes was then measured, keeping the compensating voltage the same. The piezo-Hall voltage is then given by $\frac{1}{2} V_{\text{Hac}}$, eliminating any voltage which is independent or is a symmetric function of the magnetic field (e.g., piezoresistance and

¹² M. Pollak, Rev. Sci. Instr. 29, 639 (1958).

piezo-magnetoresistance). The piezo-Hall coefficient is given by

$$\pi_l(R_H) = \frac{1}{X} \frac{1}{2} \frac{V_{Hac}}{V_{Hdc}}$$

The induced voltage was measured with the current turned off and was found to be much smaller than the piezo-Hall voltage.

E. Piezoresistance Measurements at the Boiling Point of Hydrogen and Neon

A dc stress was used for these measurements. The standard four-probe method was again used here. The sample resistance in this temperature range was quite large, so that the external resistance in the current circuit could not be kept much larger than the sample resistance (particularly for large sample-current values). This changes the sample current on the application of stress; this current change also had to be measured to obtain the piezoresistance coefficient. The piezoresistance coefficient is given by

$$\pi_l(\rho) = (\Delta V/V - \Delta I/I)/X,$$

where ΔV is the change in the voltage across the sample and ΔI is the change in the sample current on applying the stress X . The signs of ΔV and ΔI are opposite and thus $\Delta V/V$ and $\Delta I/I$ have to be added in the above expression for $\pi_l(\rho)$.

The voltage across the voltage electrodes was measured with a Keithley differential electrometer (Model 603). This instrument is equipped with a compensating voltage source. After the voltage V across the voltage electrodes was measured for zero stress, the compensating voltage was applied and adjusted for zero reading; the electrometer was then switched to one of the more sensitive ranges. The sample was then subjected to a steady stress and the value for ΔV measured. The values of I and ΔI were measured in a similar way on another Keithley electrometer, which was slightly modified to increase the voltage range for which the instrument

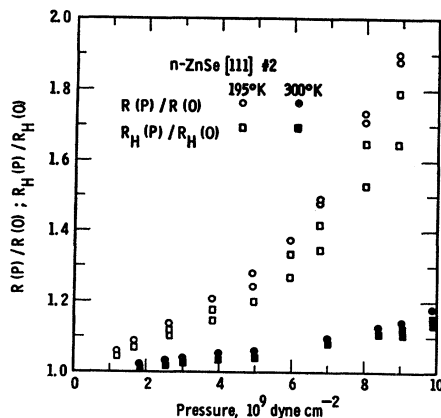


FIG. 2. $R(P)/R(0)$ and $R_H(P)/R_H(0)$ versus pressure for sample No. 2 at 195° and 300°K.

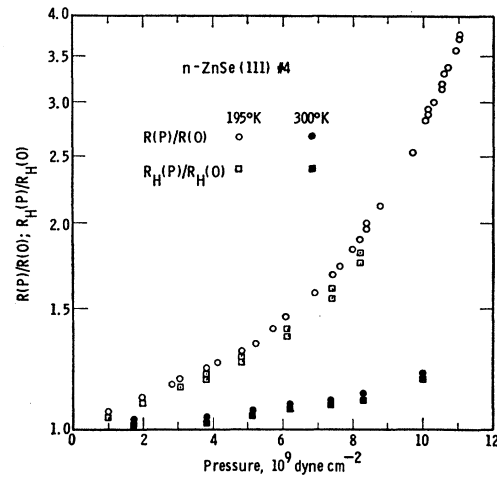


FIG. 3. $R(P)/R(0)$ and $R_H(P)/R_H(0)$ versus pressure for sample No. 4 at 195 and 300°K.

could be balanced for a zero reading. The measurements were performed for several current values. The over-all uncertainty in this measurement may be as large as $\pm 20\%$.

3. EXPERIMENTAL RESULTS

3.1 Hydrostatic-Pressure Data

The resistance and the Hall coefficient for all our samples increased with increasing pressure. The data on samples 2, 4, and 7 are shown in Figs. 2, 3, and 4, respectively. Our samples were quite inhomogeneous, as can be seen from the different Hall values at two points along the length of the samples (Table I). The pressure dependence of the Hall values at different points along the length of the samples was found to be different. The two sets of points for $R_H(P)/R_H(0)$ versus P in Figs. 2-4, represent measurements at two locations along the length of the samples. The higher set of values for $R_H(P)/R_H(0)$ represent measurements at the location

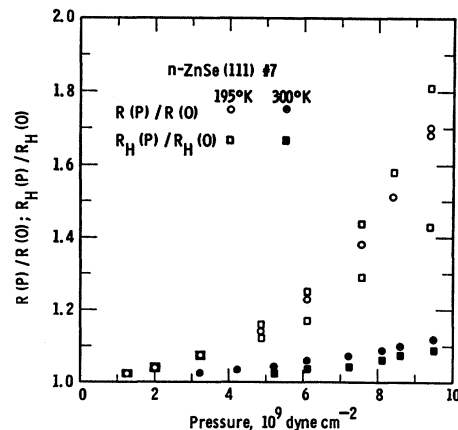


FIG. 4. $R(P)/R(0)$ and $R_H(P)/R_H(0)$ versus pressure for sample No. 7 at 195 and 300°K.

TABLE II. The piezoresistance and piezo-Hall coefficients $\pi_P(\rho)$ and $\pi_P(R_H)$ obtained from hydrostatic pressure measurements, and the longitudinal piezoresistance and piezo-Hall coefficients $\pi_l(\rho)$ and $\pi_l(R_H)$ obtained by using uniaxial stress for the *n*-ZnSe samples, in units of 10^{-12} cm² dyn⁻¹. On account of the experimental uncertainties discussed in Secs. 2.3.D and 3.1, the zeros for the values of $\pi_{\text{shear}}(\rho) = \{\pi_l(\rho) - \frac{1}{3}\pi_P(\rho)\}$ shown in the table implies $\pi_{\text{shear}} < 1 \times 10^{-12}$ cm² dyn⁻¹. The two values of various quantities in the table represent measurements at two different points on a sample and reflect sample inhomogeneities.

Sample No.	300°K				195°K				77°K	
	$-\pi_P(R_H)$	$-\pi_P(\rho)$	$-\pi_l(\rho)$	$-\pi_{\text{shear}}(\rho)$	$-\pi_P(R_H)$	$-\pi_P(\rho)$	$-\pi_l(\rho)$	$-\pi_{\text{shear}}(\rho)$	$-\pi_l(R_H)$	$-\pi_l(\rho)$
4	8	11	5	1.3	52	60	20	0		180
	10.5				47					
2	9	11.5	5.5	1.7	46	48	16	0	150	150
					39				125	
7	6	9	2.8	-0.2	20	17	5.8	0.1	73	105
					12				54	

at which the Hall value was larger. The values of $d(\ln R_H)/dP$ and $d(\ln R)/dP$ at $P=0$ are given in Table II. These values were obtained by differentiating the smooth curves R (and R_H) versus P drawn through the data points, and extrapolating the plots of $d(\ln R)/dP$ [and $d(\ln R_H)/dP$] versus P to $P=0$. The experimental uncertainty in these values is $\pm 2 \times 10^{-12}$ cm² dyn⁻¹. The following general observations are made about the data: (1) No hysteresis in the data was observed within the experimental uncertainty of less than 0.5% for the resistance measurements and less than 1% for the Hall measurements; (2) R_H and R increase with increasing pressure; (3) $d(\ln R_H)/dP$ and $d(\ln R)/dP$ increase with increasing pressure; (4) the values of $d(\ln R_H)/dP$ and $d(\ln R)/dP$ are larger at lower temperature and for samples with higher Hall values; and (5) $d(\ln R)/dP$ is larger than $d(\ln R_H)/dP$. This, however, could not be established unambiguously for very inhomogeneous samples. For example, in Fig. 4 the value of $d(\ln R_H)/dP$ at one location of sample No. 7 is larger than the value of $d(\ln R)/dP$ for that sample. However, when the Hall data is averaged over both the locations, we find that $d(\ln R)/dP > d(\ln R_H)/dP$.

3.2 Piezoresistance and Piezo-Hall Coefficients versus Temperature

The data on the longitudinal piezoresistance coefficient versus temperature are shown in Fig. 5. The data in this figure have been corrected for the dimensional changes. The values for $\frac{1}{3}\pi_P(\rho)$ and $\frac{1}{3}\pi_P(R_H)$ at 300 and 195°K taken from the pressure data are also shown. The values of $\frac{1}{3}\pi_P(R_H)$ here represent the average of the two values obtained at the two sets of probes for each sample (Table II). The piezo-Hall data on samples No. 4 and 7 are also shown in the figure. The two different values of $\pi_l(R_H)$ shown at 77°K for each sample are the values obtained at the two sets of probes. The higher value for $\pi_l(R_H)$ was obtained at the location with a higher Hall value. The different values of $\pi_l(R_H)$ at two locations along the length of a sample result from the inhomogeneity of the samples. Meaningful data on $\pi_l(R_H)$ could not be obtained at temperatures above 100°K, because the effect becomes quite small and the

precision of the measurement is quite poor for $\pi_l(R_H) < 10 \times 10^{-12}$ cm²/dyn. The following general observations are made about the data: (1) $\pi_l(\rho)$ and $\pi_l(R_H)$ decrease rapidly with increasing temperature between 77 and 300°K; (2) $\pi_l(\rho)$ tends towards T^{-1} dependence in the low-temperature region. We do not have enough data to make a definitive estimate about the temperature dependence of $\pi_l(\rho)$ in this temperature range; (3) the piezoresistance and piezo-Hall effects are smaller for samples with lower Hall coefficients; (4) $\pi_l(\rho) = \frac{1}{3}\pi_P(\rho)$ within the experimental uncertainty. This implies $\pi_{\text{shear}} \approx 0$. The data at 195°K show this precisely. The numbers at 300°K are small to establish this precisely. However, it is true within the experimental uncertainty. (5) $\pi_l(\rho)$ is larger than $\pi_l(R_H)$. This result is consistent with our observations made about the pressure data, and implies a decrease in the electron Hall mobility with compressional stress or hydrostatic pressure. However,

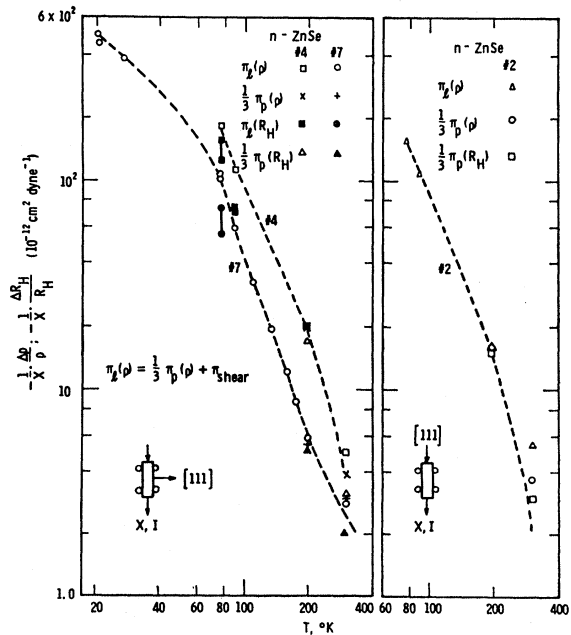


FIG. 5. Piezoresistance and piezo-Hall effect versus temperature for the three samples.

the inhomogeneities in our samples indicated by the Hall and resistivity measurements (Table I) can probably account for some of the observed difference in the $\pi_l(\rho)$ and $\pi_l(R_H)$ values. As a qualitative argument, let us consider the case where the electron concentration varies mostly along the length and very little along the cross section of the samples. In that case, the major contribution to the resistance comes from the high-resistivity regions, whereas the Hall voltage is derived primarily from the low-resistivity regions of the samples. The first part of this statement is self-evident. The argument concerning the Hall voltage is as follows: If we consider two neighboring regions of a sample, characterized by the electron concentrations n_1 and n_2 , then the effective Hall voltage can be approximated by considering a parallel connection of two generators, characterized by the generating voltages $V_1=(k/n_1)$ and $V_2=(k/n_2)$, and the internal resistances $R_1=(c/n_1)$ and $R_2=(c/n_2)$, respectively, where k and c are constants. Then the resulting voltage, which represents the observed Hall voltage, is given by $V_H=(V_1R_2+V_2R_1)/(R_1+R_2)$. Let us assume $n_1>n_2$. Then we find that V_H is closer to V_1 than to V_2 , thus proving the above statement. Since the strain is uniformly distributed, the experimental values for the resistance and the piezoresistance effects would represent mainly the contributions from the high-resistivity regions, and the piezo-Hall values mainly from the low-resistivity regions. We further observe in Table II that the samples with higher resistivity and Hall values exhibit higher piezoresistance and piezo-Hall values. Thus the observation $\pi_l(\rho)>\pi_l(R_H)$ could also result from the inhomogeneities present in our samples.

3.3 Resistance versus Temperature Data for Sample No. 7

The resistance of sample No. 7 was measured down to 15°K. The value of the slope for the best straight line drawn through the data $\ln\rho$ versus T^{-1} was found to be 0.024 eV. Our samples were heavily compensated, so that we can assume $n\ll N_a$. This is certainly true in the low-temperature range. Thus, Eq. (6) rather than Eq. (8) of Sec. 4.2 below would be assumed to give correct electron concentration. If we further assume for the temperature dependence of the electron mobility $\mu\sim T^{3/2}$ (which perhaps is not unreasonable around 20°K), then the slope of the best straight line drawn through $\ln(\rho T^3)$ versus T^{-1} , implies the value for the donor ionization energy $\epsilon_d\approx 0.020$ eV. If we assume that the electron mobility is independent of temperature, then we obtain a value for $\epsilon_d\approx 0.022$ eV. Evidently, there is some uncertainty in our estimate for the value of ϵ_d due to the uncertainty in our assumption about the temperature dependence of the electron mobility. However, the value for $\epsilon_d\approx 0.020$ eV is perhaps more correct.

4. DISCUSSION

4.1 Discussion of Results

The result $\pi_{\text{shear}}\approx 0$ is suggestive of the (000) conduction band for this material and is consistent with other work.^{1,3-6} The small decrease in the Hall mobility with pressure which manifests itself in the result $\pi_P(\rho)>\pi_P(R_H)$ is at least partly due to the increase in the electron effective mass m_e^* with pressure, which in turn results from the increase in the direct energy gap.

The gross features of our results concerning the large changes in the resistance and the Hall coefficients of the samples as a function of pressure can be qualitatively explained on the basis of the postulate that the ionization energy of the donor states important in our n -ZnSe samples increases appreciably with pressure. Large pressure effects on the resistance and Hall coefficient have been observed in other materials, e.g., n -GaAs,¹³⁻¹⁵ n -CdTe,^{16,17} and n -GaSb,^{18,19} and have been successfully explained as due to the strong pressure dependence of their respective donor ionization energies. The lowest conduction-band minimum for all these materials lies at $k=(000)$. In order to explain the large pressure dependence of the donor ionization energies in these materials, Paul²⁰ put forward the postulate that these pressure-sensitive donor states are formed from the higher-lying subsidiary conduction-band wave functions or at least there is a considerable admixture of higher-lying conduction-band functions to the donor states. The experimental values of $(d\epsilon_d/dP)$ for n -GaAs and n -CdTe were found to be consistent with the assumption that the donor states responsible for the large pressure effects in these materials are formed from the (100) conduction band. However, the experimental values of $(d\epsilon_d/dP)$ for the two materials could also be consistent with the assumption that the donor states are formed from the valence-band wave functions. This difficulty of distinguishing between the two possibilities arises for almost all the III-V and II-VI compounds because the energy separation between the valence band and the (100) conduction band in these materials is relatively insensitive to pressure.^{2,15,21} The experimental evidence in support of Paul's hypothesis comes from a series of pressure experiments by Kosicki *et al.*^{18,19} on n -GaSb containing different doping elements of group VI of the periodic table (i.e., Te, Se, S). They found that the

¹³ R. J. Sladek, in *Proceedings of the International Conference on the Physics of Semiconductors, Paris, 1964* (Dunod Cie., Paris, 1964), p. 545.

¹⁴ R. J. Sladek, *Phys. Rev.* **140**, A1345 (1965).

¹⁵ A. R. Hutson, A. Jayaraman, and A. S. Coriell, *Phys. Rev.* **155**, 786 (1967).

¹⁶ A. G. Foyt, R. E. Halsted, and W. Paul, *Phys. Rev. Letters* **16**, 55 (1966).

¹⁷ A. Sagar and M. Rubenstein, *Phys. Rev.* **143**, 552 (1966).

¹⁸ B. B. Kosicki and W. Paul, *Phys. Rev. Letters* **17**, 246 (1966).

¹⁹ B. B. Kosicki, W. Paul, A. J. Strauss, and G. W. Iseler, *Phys. Rev. Letters* **17**, 1175 (1966).

²⁰ See the discussion by W. Paul on paper by R. J. Sladek in Ref. 13.

²¹ R. Zallen and W. Paul, *Phys. Rev.* **134**, A1628 (1964).

pressure dependence of resistance is a strong function of the type of donor impurity present in the material. They interpret their data on the basis that a donor impurity in a semiconductor may have a number of energy levels, each of which is associated primarily with one of the conduction bands, and is fixed in energy relative to that band as a function of pressure. They conclude from their data that the observed energy levels in GaSb for the sulfur, selenium, and tellurium impurities are associated primarily with the (100), (111), and (000) conduction bands, respectively.

In the next section, we shall analyze our piezoresistance and pressure data for *n*-ZnSe, in order to estimate the values for ϵ_d and $(d\epsilon_d/dP)$, and further attempt to determine the nature of the donor states responsible for the large pressure effects in this material.

4.2 Estimate for $(d\epsilon_d/dP)$ from the Pressure Data

When classical statistics can be used for the electrons in the conduction band, we have

$$n = (N_d - N_a) - N_d(1 + N_c'/n)^{-1}, \quad (1)$$

where n is the electron concentration in the conduction band, and N_d and N_a are the donor and the acceptor concentrations, respectively, $N_c' = N_c g^{-1} e^{-\epsilon_d/kT}$, g is the degeneracy factor for the donor level, ϵ_d is the donor ionization energy, and $N_c = 2(2\pi m_e^* kT/h^2)^{3/2}$. We shall further assume that the observed piezoresistance in our samples is due to the pressure dependence of ϵ_d , and shall neglect all "minor" effects, so that

$$\pi_P(\rho) = -d(\ln\rho)/dP = d(\ln n)/dP.$$

In the range of pressure, temperature, and the amount of compensation in the sample, where the condition $N_c'(N_d - N_a) \ll (N_a + N_c')^2$ is justified, Eq. (1) approximates to the solution

$$n = (N_d - N_a)(1 + N_a/N_c')^{-1}. \quad (2)$$

The expression for $\pi_P(\rho)$ for this approximation is given by

$$\pi_P(\rho) = -\left(\frac{1}{kT} \frac{d\epsilon_d}{dP}\right) \left(1 + \frac{N_a}{N_c'}\right)^{-1}. \quad (3)$$

If we further restrict the solution to the situation where $N_c' \gg N_a$, we have

$$\pi_P(\rho) = -\left(\frac{gN_a}{N_c}\right) \left(\frac{d\epsilon_d}{dP}\right) \frac{e^{\epsilon_d/kT}}{kT}. \quad (4)$$

According to this equation, the value of $\pi_P(\rho)$ approaches zero in the high-temperature range. This can also be seen from Eq. (2), which, in the high-temperature range $kT \gg \epsilon_d$ and when $N_c' \gg N_a$, reduces to

$$n = (N_d - N_a) \quad (5)$$

and gives

$$\pi_P(\rho) = 0.$$

In the temperature and pressure range where $\epsilon_d \gg kT$ is justified, N_c' will be small. For the partially compensated samples, in the low-temperature (or high-pressure) range, we can have $N_c' \ll N_a$, so that the condition $N_c'(N_d - N_a) \ll (N_a + N_c')^2$ is still satisfied, and Eq. (2) is valid. Thus, for the case $N_c' \ll N_a$, the solution approximates to²²

$$n = \left(\frac{N_d - N_a}{N_a}\right) g^{-1} N_c e^{-\epsilon_d/kT}. \quad (6)$$

The expression for $\pi_P(\rho)$ in this range is given by

$$\pi_P(\rho) = -\frac{1}{kT} \left(\frac{d\epsilon_d}{dP}\right). \quad (7)$$

In case the samples have negligible compensation, i.e., $N_a \ll N_d$, the condition $N_c'(N_d - N_a) \ll (N_a + N_c')^2$ is justified only in the range of temperature, pressure, and the impurity concentrations where $N_c' \gg N_a$. In that case, Eqs. (1)–(5) would still be applicable. However, in the low-temperature range $kT \ll \epsilon_d$, where $N_c' \ll N_a$, we cannot use this approximation, and Eqs. (6) and (7) are no longer valid. The solution of Eq. (1) in the low-temperature range where $N_a \ll N_c' \ll N_d$ is given by

$$n = (N_d N_c g^{-1})^{1/2} e^{-\epsilon_d/2kT} \quad (8)$$

and

$$\pi_P(\rho) = -\frac{1}{2kT} \left(\frac{d\epsilon_d}{dP}\right). \quad (9)$$

Our samples are quite heavily compensated, so that in the low-temperature range $kT \ll \epsilon_d$, we have $N_c' \ll N_a$. Thus the Eqs. (6) and (7) [rather than Eqs. (8) and (9)] are applicable for our samples at the pressure and temperature where the condition $kT \ll \epsilon_d$ is applicable. We have pressure data only at 195 and 300°K, where at normal pressure $\epsilon_d \approx kT$. Even in the high-pressure range the data at 300°K do not approach the condition $\epsilon_d \gg kT$. The pressure data at 195°K seem to be approaching the condition $\epsilon_d \gg kT$ in the high-pressure range, but do not fully satisfy this condition even at the highest pressure of our experiment. The value of $(d \ln R/dP)$ is steadily increasing for all samples even at our highest pressures. However, we can estimate the lower limit for the value of $(d\epsilon_d/dP)$ from our data. The data on sample No. 4 (Fig. 3) yield the largest value for $(d \ln R/dP)$ compared to the other samples. The largest

²² According to Eq. (6), the resistivity of the material in the range $\epsilon_d \gg kT$ is a function of N_d/N_a , whereas it is a function of $(N_d - N_a)$ in the range $\epsilon_d \ll kT$ (Eq. 5). The pressure data on *n*-CdTe by Foyt *et al.* (Ref. 16) showed the interesting feature that the high-pressure resistivity (in the range $\epsilon_d \gg kT$) of all the samples became identical, while the resistivity values for the samples in the low-pressure range differed by three orders of magnitude, thus indicating that all those samples had the same N_d/N_a value, although the electron concentrations in the samples at normal pressure differed by orders of magnitude. This tendency for self-compensation in the II-VI compounds is quite well known.

value of $(d \ln R/dP) \approx -360 \times 10^{-12} \text{ cm}^2/\text{dyn}$ is obtained for this sample at the highest pressure up to which the data were taken. Thus from Eq. (7) we have $(d\epsilon_d/dP) \geq kT \times 360 \times 10^{-12} \approx +5.2 \times 10^{-12} \text{ eV/dyn cm}^{-2}$. If we assume that the donor wave functions are formed strictly from the valence-band function, then, from the results of Edwards *et al.*,¹ we should have $(d\epsilon_d/dP) \approx +6 \times 10^{-12} \text{ eV/dyn cm}^{-2}$. The other possibility—that the donor states are formed from the (100) conduction band—leads to $(d\epsilon_d/dP) \approx +8 \times 10^{-12} \text{ eV/dyn cm}^{-2}$. We cannot distinguish between the two possibilities from our experimental result $(d\epsilon_d/dP) \geq +5.2 \times 10^{-12} \text{ eV/dyn cm}^{-2}$. We can only conclude from this data that there is considerable contribution from some band or bands other than the (000) conduction band to the donor state functions we are concerned with here.

4.3 Piezoresistance versus Temperature

Our piezoresistance data is mostly between 77 and 300°K. The values of $\pi_i(\rho)$ between 195 and 300°K are generally less than $10 \times 10^{-12} \text{ cm}^2/\text{dyn}$, in which case both the experimental errors and the “minor” effects become quite important. Thus, we shall examine the data only between 77 and 195°K. The condition $N_c' \gg N_a$ is perhaps not unreasonable in this temperature range, and thus Eq. (4) would be applicable. The data of Fig. 5 are replotted in Fig. 6 in the form $\log \pi_i T$ versus T^{-1} . We have fairly complete data on sample No. 7. We find that the data on this sample give a good straight-line fit except for the points near 195°K, where a good fit is not expected because, near this temperature, $\pi_i(\rho) \approx -5 \times 10^{-12} \text{ cm}^2/\text{dyn}$, and both the “minor” effects and the experimental errors are relatively large. The slope of this straight line yields a value $\epsilon_d \approx 0.019 \text{ eV}$. This is in excellent agreement with the value $\epsilon_d \approx 0.020 \text{ eV}$ derived from the resistance-versus-temperature data in the low-temperature range. It may be pointed out that both these measurements give us the value of ϵ_d at 0°K, assuming linear temperature dependence for ϵ_d within the range of temperature of each experiment. This result further justifies our assumption $N_c' \ll N_a$ and the use of Eq. (6) rather than Eq. (8) for this sample around 15°K. Such an excellent agreement between the values obtained from the two different measurements is perhaps somewhat fortuitous, due to the uncertainty in the assumption about the temperature dependence of the electron mobility, necessary to estimate the value for ϵ_d from the ρ -versus- T data. However, no such assumption is required to determine ϵ_d from the piezoresistance data. Thus, we believe that the piezoresistance data yields a more reliable estimate for ϵ_d .

We do not have enough data points for samples No. 2 and 4 to justify drawing straight lines through them. However, the values for $\pi_i(\rho)$ at 195°K are large enough ($\approx -20 \times 10^{-12} \text{ cm}^2/\text{dyn}$) for these samples, so that the uncertainties involving “minor” effects and the experi-

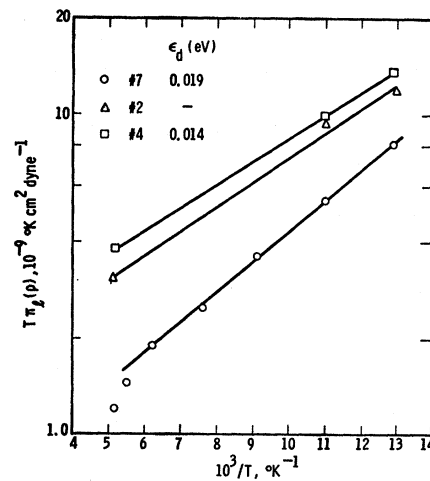


FIG. 6. $\log T\pi_i(\rho)$ versus T^{-1} for the three samples.

mental errors are still small and can be ignored. The straight line through the points for sample No. 4 yield a value for $\epsilon_d \approx 0.014 \text{ eV}$. This value is about 25% smaller than the value obtained for sample No. 7. This difference could be partly due to the large uncertainty in the determination of the slope of the best straight line drawn through the very limited piezoresistance data for this sample. This difference in ϵ_d values, if real, cannot be simply explained as due to the difference in donor concentration in our samples, because our result indicates a lower value for ϵ_d for the samples with lower electron concentration. However, our samples have varying amounts of compensation, and lower electron concentration does not by itself imply a lower donor concentration in our samples.

The piezoresistance of sample No. 7 was measured also at the boiling points of hydrogen and neon. In this temperature range, $\epsilon_d \gg kT$, and Eq. (7) is applicable, so that $(d\epsilon_d/dP) = -3kT\pi_i(\rho) \approx +2.6 \times 10^{-12} \text{ eV/dyn cm}^{-2}$. This value is in disagreement with the result $(d\epsilon_d/dP) \geq +5.2 \times 10^{-12} \text{ eV/dyn cm}^{-2}$ obtained from the high-pressure data for sample No. 4 at 195°K. If Eq. (9) rather than Eq. (7) were assumed to be valid for sample No. 7, then the low-temperature piezoresistance data would yield a value for $(d\epsilon_d/dP)$ which would be in better agreement with the value derived from the high-pressure data for sample No. 4 at 195°K. However, this would imply $N_a \ll N_c'$ for sample No. 7 around 15°K, which cannot be justified, if for no other reason than the state of the art of preparing ZnSe at the present time. Furthermore, such an assumption, when applied to the ρ versus T data in the low-temperature range would result in a value for ϵ_d which is inconsistent with the value derived from the $\pi_i(\rho)$ versus T data for this sample. The analysis of the data on $\pi_i(\rho)$ versus T [Fig. 6 and Eq. (4)] is free from such an uncertainty. We can safely state that any assumptions about the compensation in the samples made for the analysis of

the data at low temperature would not be valid if they yield results which are inconsistent with the result obtained from the analysis of the $\pi_i(\rho)$ -versus- T data [Fig. 6 and Eq. (4)]. Evidently, the simple model based on the pressure dependence of a single donor level does not suffice to explain the piezoresistance data around 20°K. A detailed experimental investigation in this temperature range is required before any firm explanation can be proposed for this disagreement between the low- and the high-temperature piezoresistance data.

5. CONCLUSION

The result $\pi_{\text{shear}} \approx 0$ indicates that the lowest conduction-band minimum for this material is situated at $\mathbf{k} = (0,0,0)$, and is in agreement with other work.^{1,3-6} The piezo-Hall and piezoresistance effects can be

qualitatively explained on the basis of the simple model that the donor ionization energy ϵ_d increases appreciably with pressure. The value $\epsilon_d \approx 0.019$ eV determined for one sample from the data on $\pi_i(\rho)$ versus T is in excellent agreement with the value $\epsilon_d \approx 0.020$ eV estimated from the low-temperature data on ρ versus T . The result $(d\epsilon_d/dP) \geq +5.2 \times 10^{-12}$ eV/dyn cm⁻² derived from the pressure data at 195°K suggests that there is considerable contribution from some band other than the (000) conduction band to the donor state functions. The piezoresistance data around 20°K, when simply interpreted on the basis of the pressure dependence of the ionization energy of the single donor level, yield $(d\epsilon_d/dP) \approx +2.6 \times 10^{-12}$ eV/dyn cm⁻², in disagreement with the estimate obtained from the pressure data at 195°K.

Low-Field Mobility and Galvanomagnetic Properties of Holes in Germanium with Phonon Scattering

P. LAWAEZT

Physics Laboratory III, The Technical University of Denmark, Lyngby, Denmark

(Received 3 June 1968)

A theoretical calculation of the low-field galvanomagnetic properties of holes in Ge has been carried out incorporating all relevant details of the band structure. The scattering is limited to acoustic and optical phonons and is described by the deformation potentials a , b , d , and d_0 . For pure acoustic scattering, no overall consistency is found between available galvanomagnetic data and deformation potentials derived directly from experiments on strained Ge. The discrepancies may be ascribed to ionized-impurity scattering, but at higher temperatures where optical phonon scattering is operative, the deviations are still appreciable. We are led to conclude that the deformation-potential theory of phonon scattering needs reconsideration, and a nontrivial correction is pointed out.

I. INTRODUCTION

ALTHOUGH the electrical transport properties of holes in Ge are more or less qualitatively understood, their quantitative interpretation is still far from satisfactory.¹ The difficulties encountered in this connection are primarily due to the complicated energy spectrum of holes in the vicinity of the degenerate valence-band edge, which consists of the two bands

$$E_{1,2}(\mathbf{k}) = Ak^2 \pm [B^2k^4 + C^2(k_x^2k_y^2 + k_y^2k_z^2 + k_z^2k_x^2)]^{1/2}. \quad (1.1)$$

The principal aim of the present work is to calculate the low-field galvanomagnetic parameters mobility, Hall factor, and magnetoresistance, avoiding any serious approximations in the band structure or its effects on scattering, so that it might be possible to establish a

quantitative correlation between some important transport properties.

The scattering mechanisms will be limited to acoustic and optical phonons, and are treated on the basis of the deformation-potential theory developed by Bir and Pikus.² In this theory, the hole-phonon interaction is determined by the four deformation potentials a , b , d , and d_0 . Of these, the first three, pertaining to the acoustic scattering, also describe the change in the valence-band structure with static strain³ and, consequently, they enter the theory of a large number of phenomena pertaining to the valence band. d_0 is connected with the optical phonon scattering and appears only in the theory of transport phenomena.

The previous theories of low-field transport may all be regarded as simplifications of the general case intro-

¹ E. G. S. Paige, *Progress in Semiconductors* (Heywood and Co., Ltd., London, 1964), Vol. 8, p. 1. This review article discusses most of the earlier experimental and theoretical work on electrical transport properties of holes in Ge.

² G. L. Bir and G. E. Pikus, *Fiz. Tverd. Tela* **2**, 2287 (1960) [English transl.: *Soviet Phys.—Solid State* **2**, 2039 (1961)]. A similar theory was worked out independently by M. Tiersten, *IBM J. Res. Develop.* **5**, 122 (1961).

³ G. E. Pikus and G. L. Bir, *Fiz. Tverd. Tela* **1**, 1624 (1959) [English transl.: *Soviet Phys.—Solid State* **1**, 1502 (1960)].